Research Article

Petrochemical Wastewater Treatment by Eggshell Modified Biochar as Adsorbent: Atechno-Economic and Sustainable Approach

Andy G. Kumi [ID],[1] **Mona G. Ibrahim** [ID],[1,2] **Manabu Fujii** [ID],[1,3] **and Mahmoud Nasr** [ID][1,4]

[1]*Environmental Engineering Department, Egypt-Japan University of Science and Technology (E-JUST), New Borg El-Arab City, Alexandria 21934, Egypt*
[2]*Environmental Health Department, High Institute of Public Health, Alexandria University, Alexandria 21544, Egypt*
[3]*Civil and Environmental Engineering Department, Tokyo Institute of Technology, Meguro-Ku, Tokyo 152-8552, Japan*
[4]*Sanitary Engineering Department, Faculty of Engineering, Alexandria University, P.O. Box 21544, Alexandria 21526, Egypt*

Correspondence should be addressed to Mahmoud Nasr; mahmmoudsaid@gmail.com

Petrochemical industrial wastewater (PIW)contains toluene and xylene (TX), and various organic and inorganic pollutants, causing severe risks to human health if improperly released into the environmental matrices. For the long-term reliability of environmental conservation, this study illustrates the interlinkage between PIW treatment and the three pillars of sustainable development. Sewage sludge biochar was modified with eggshell, showing a relatively high fixed C content (increase in carbonization degree), and small O/C and N/C ratios. The prepared biochar was employed for TX adsorption in mono-component solutions, giving removal efficiencies of 79.1% (T) and 86.6% (X), at pH =10, adsorbent dosage =2 g/L, and $C_o =$ 40 mg/L within 60 min. The main adsorption mechanism was physisorption, including precipitation/pore-filling, π-π dispersive interaction, and van der Waals force. The modified biochar also treated real PIW under five adsorption/regeneration cycles, providing essential steps toward large-scale applications. According to an economic feasibility estimation, the biochar application for treating 1 m^3 of PIW would offer a payback period of 6.9 yr. The study outputs could be linked to the restoration of water-related ecosystems, biochar modification for industrial applications, and climate change mitigation, adopting the 2030 agenda and its sustainable development goals (SDGs).

1. Introduction

Petrochemical manufacturing industries generate large amounts of wastewater composed of aromatic hydrocarbons and organic solvents, e.g., toluene and xylene (TX) [35]. The TX compounds of petrochemical industrial wastewater (PIW) are considered slowly biodegradable and highly toxic, imposing harmful and emerging threats on human health [31]. The unsafe disposal of these hydrocarbons would damage the human organs and central nervous system, or could even cause death at high doses [24]. Because PIW should be managed properly using sustainable and feasible pathways, its treatment should be investigated regarding the environmental and economic points of view.

Various physicochemical methods have been adopted to treat PIW, providing a rapid process accompanied by convenient operation and control. Unlike in biological systems, the physicochemical-based processes could withstand fluctuating temperature patterns and complex discharges within a shorter treatment time [9]. Among thephysicochemical treatment techniques, adsorption is becoming a cost-effective, simple, andenvironmentally friendly option to mitigate PIW-related pollution [1]. Adsorption is not considered an energy-intensive technique because it does not usually require aeration, heating, and/or mixing [16]. Adsorption does not also suffer from sludge handling and management due to the utilization of low quantities of chemical reagents, providing an economically feasible approach [28]. Previous

researchers have investigated the treatment of PIW by adsorption onto crumb rubber [3], graphene [16], Na-P1 zeolite [5], silica [24], biocomposite [1], carbon nanotubes [4], and solid waste biochar [15]. Based on these studies, the adsorbent should be abundantly available, eco-friendly, and prepared with a cheap materialfor providing a stand-alone wastewater treatment system.

In most developing countries, wastewater treatment processes generate large amounts of sewage sludge that could pose serious burdens tothe environment (soil and groundwater) [25]. A proper and smart waste (e.g., sludge) management system should be outlined according to the sustainable development goals (SDGs), tackling multiple environmental, economic, and social aspects [8]. Waste sludge could be utilized as a renewable biomass to produce biochar (a carbon-rich material) via pyrolysis [27]. Biochar has been employed as an innovative and effective adsorbent for removing aqueous contaminants such as complex organic compounds fromindustrial effluents [11]. However, under improper sludge pyrolysis, biochar might be unable to capture large amounts of pollutants due to the associated insufficient surface area and poor porosity [14]. Adding food residues and optimizing the pyrolysis temperature are efficient options to modifythe texture, surface functional groups, molecular structure, and pore-size distribution of biochars [22, 32]. For example, eggshell wastescould be utilized for providing multiple functional groups and mineral components (calcite) to biochars [6]. This pattern would enhance the intrinsic features and pore structure of biochars to improve the adsorption performance.

A significant gap exists in the literature regarding the relationship between biochar manufacturing, SDGs, and economic feasibility, which should be comprehensively addressed. Hence, this study is the first toillustrate the interlinkage between PIW treatmentand the three pillars of sustainability via the techno-economic feasibility of a modified biochar adsorbent. In particular, the study objectives are fourfold (i) characterize biocharproduced from sludge and eggshell wastes, (ii) determine optimum pyrolysis temperature, effects of adsorption conditions on TX removal, and suggested adsorption mechanisms, (iii) test the synthesized biochar for treating real PIW under successive adsorption/ regeneration cycles, and (iv) highlight the achievable SDGs, environmental considerations, and economic feasibility associated with the study outputs.

2. Materials and Methods

2.1. Wastewater Preparation/Collection.
The synthetic medium was prepared by initially dissolving calculated volumes of each of T and X compounds in a small amount of methanol, not exceeding 1% in the stock solutions. The standard stock solutions (1000 mg/L of each of T and X) were dilutedwith appropriate amounts of distilled water to prepare mono-component systems (T and X: 40 – 200 mg/L). The suspension pH was regulatedby adding either 0.1 M NaOH or 0.1 M HCl solutions. For treatingreal PIW, a petrochemical industry situated in Alexandria, Egypt, was selected to collect the wastewater samples. The received

PIW samples were directly used in the adsorption treatment assays without further adjustments. All solutions were stored in glass-stoppered bottles under the dark condition at 4°C. All reagents and solvents were of analytical grade (Sigma–Aldrich; >99% purity) and used without further purification.

2.2. Biochar Adsorbentpreparation.
Sewage sludge was collected from the Alexandria East wastewater treatment plant (WWTP) located in Alexandria, Egypt. All the sludge samples were oven-dried (100°C for 24 hrs), and then screened using a 60-mesh sieve. Sludge pyrolysis was performed in an oxygen-deprived condition using a muffle furnace (Asahi Rika tabletop, AMF-25 N, Japan) to prepare the raw biochar (BC) material. The pyrolysis temperatures were investigated at300, 350, 400, 450, 500, and 550°C with a 5°C/min heating rate for 60 min, based on the methods of earlier reports [2, 39]. These biochars were labelled as BC300, BC350, BC400, BC450, BC500, and BC550, respectively. The raw biochars (300–550°C) were examined for TX adsorption, and the best pyrolysis temperature was selected to prepare eggshell-modified biochar (EMBC), following our previous study [18].

2.3. Adsorption Experiment.
In the first experiment, single-component sorption assayswere performed in 250 mL flasks under 100 rpm stirring rate at room temperature (25 ± 2°C). The influences of adsorption factorson TX removal were statistically investigated using a one-factor-at-a-time method. Briefly, the first run was conducted by varying the pH values from 2 to 12 at adsorbent dosage = 1 g/L and C_o = 100 mg/L within 60 min. The optimized pH was used in the second assay at C_o = 100 mg/L for 60 min with increasing the adsorbent dosagefrom 2 to 10 g/L. Theseoptimum pH and dosage values were further used to operate the adsorption system for 60 min with varying C_o from 40 to 200 mg/L.The optimum pH, adsorbent dosage, and C_o were used in the fourth experimental assay to investigate the influence of adsorption time (5–240 min) on TX removal. The measured TX concentrations were used to estimate the adsorption performance in Eqs. (1) and (2).

$$R = \frac{C_o - C_e}{C_o} \times 100 \tag{1}$$

$$q = (C_o - C_e) \times \frac{V}{m} \tag{2}$$

where R is the adsorbate removal percentage (%), q is uptake capacity (mg adsorbate/g biochar), C_o and C_e are the initial and equilibrium adsorbate concentrations (mg/L), respectively, m is biochar mass (g), and V is the flask working volume (L).

The second experiment was conducted to determine the adsorption performance and stability of biochar for real PIW treatment. For this purpose, five adsorption/regeneration cycles were conducted to assess biochar reusability. Before each re-adsorption trial, the utilized biochar was washed with methanol and then dried overnight at 105°C. All experiments were conducted in triplicate, and the average results were recorded.

TABLE 1: Physiochemical, BET surface area and pore properties of biochars produced at various pyrolysis temperatures (300–550°C).

Properties	BC 300	BC 350	BC 400	BC 450	BC 500	BC 550
Yield (wt. %)	66.10	54.20	45.82	38.60	38.55	38.09
pH	7.87	8.13	8.49	8.68	8.76	8.88
C (w/w %)	84.79	77.55	73.4	69.28	65.56	67.43
N (w/w %)	5.90	5.56	5.23	4.71	4.18	4.16
O (w/w %)	18.09	17.82	15.68	12.62	9.86	6.73
C/N ratio	14.37	13.95	14.03	14.71	15.68	16.21
O/C ratio	0.21	0.23	0.21	0.18	0.15	0.10
S (w/w %)	0.92	0.48	2.13	3.82	2.94	1.79
Ca (w/w %)	3.40	3.79	7.69	7.81	7.62	9.00
BET (m^2/g)	0.227	0.282	1.266	22.680	27.240	52.210
Total pore volume (cm^3/g)	0.00562	0.00745	0.00919	0.02962	0.01087	0.03238
Average pore size (nm)	14.00	12.60	12.20	1.29	1.27	1.23

2.4. Analytical Analysis. Biochars were characterized for their specific surface area and pore-size distribution using the methods of Brunauer–Emmett–Teller (BET) and the Barrett–Joyner–Halenda (BJH) [23].BELSORP-mini II instrument (BEL Japan, Inc.) was assigned for measuring the N_2 adsorption–desorption isotherms at 77 K, following Shaheen et al. [27]. Proximate analysis and pH of biochars were determined as adapted from Fidel et al. [10]. X-ray diffractometer (XRD) (Shimadzu Xlab 6100, Kyoto, Japan) was used to analyze the biochar crystallinity over a 2θ range of 5–80° (0.02° step size @ 12°C/min). The XRD instrument was operated with Cu-Kα radiation ($\lambda = 1.5406$ Å) at 40 kV and 30 mA.A Fourier Transform Infrared (FTIR) spectroscopy (Vertex 70, Bruker Optics Inc., Ettlingen, Germany) was used to detect the shift in peak wavenumbers associated with the adsorption process. The change in FTIR bands was recorded over the 4000–400 1/cm region. The surface morphology of biochars was characterized by scanning electron microscopy (SEM, JSM-6010LV JEOL, Tokyo, Japan). Energy Dispersive X-ray analysis in conjunction with the SEM instrument was employed to provide information ofthe biochars' elemental composition (e.g., C, N, and O), following the procedures reported elsewhere [2, 15]. For identifying the benzene, T, ethylene, and X components, the liquid samples were treated through a 0.22 μm filter (Whatman syringe filters). The resulting filtrates were analyzed byGas Chromatography-Mass Spectrometry (GC-MS), with a QP2010 PLUS system (Shimadzu, Japan) and helium as a carrier gas.

3. Results and Discussion

3.1. Biochar Characterization

3.1.1. Biochar Yield Andnutrient Content. Table 1 represents the variation in the properties and nutrient availability of biochars under different pyrolysis temperature conditions. The pyrolysis temperature substantially affected the yield of biochars. For instance, at 300°C the biochar yield was 66.1%, representing about 2-folds the yield at 450°C. The negative correlation between the biochar yield and the pyrolysis temperature could be ascribed to the thermal decomposition and gasification of the sludge components, such as volatile compounds and other non-carbon elements [32]. The volatilization of organic acids under high-temperature conditions also contributed to the rise in pH values (Table 1). Shaaban et al. [26] reported that elevated pyrolysis temperatures would increase the amounts of basic OH groups on the biochar surface, accompanied byeliminating various acidic functional groups. Increasing the total surface basicity of biochars, owing to organic acid decomposition, at elevated pyrolysis temperatures has also been verified [25]. However, increasing the pyrolysis temperature to550°C provided an insignificant ($p > 0.05$) impact on the biochar yield, assigning that the carbonization process was almost completed.

Table 1 also revealed that biochars contained nutrient species (e.g., N, S, and Ca) that have probably been embedded in the components of the collected sewage sludge. The reduction of the C, N, and O fractions for biochars pyrolyzed at 300–550°C could be ascribed to the pyrogenic decompositions and emission of volatile matters at elevated temperatures [26]. Hence, a high proportion of nutrientswould be maintained in biochars synthesizedat low pyrolysis temperatures. The variation of the nitrogen properties with temperature (Table 1) could be assigned to the loss of volatile nitrogen species, such as ammonia or volatile amines, obtaining stable pyridine compounds at elevated temperatures [14]. Moreover, the C/N ratio of the biochar products varied as a result of carbonization along with the conversion and transformation of the organic nitrogen fractions [30]. The change in the O/C ratio between 0.10 and 0.23 could be linked to the degree of polarity [2], attaining a minimum O/C ratio of 0.10 at 550°C. A low O/C ratio at elevated pyrolysis temperatures is an indication of the high aromatic nature (i.e., the aromatic linkages were more stable) of the investigated biochars [30]. This O/C range is comparable to O/C 0.07 – 0.27 for biochar-based crop residues [2], but lower than O/C 0.59 – 0.71 for biochars obtained from digested sludge [32].

3.1.2. BET Surface Area. Increasing the pyrolysis temperature from 300 to 550°C provided a positive impact on

theBET surface area, which improved from 0.23 to 52.21 m^2/g, respectively (Table 1). This BET surface area is higher than that (2.0–3.2 m^2/g) of biochar prepared from poultry litter [30]. For the preparation of rice husk biochars [28], the BET surface area was increasedfrom 45.2 to 193.1 m^2/g with raising the pyrolysis temperature from 500 to 700°C, respectively. Comparable patterns were noticed for the total pore volume (Table 1), which could be linked to a high degree of carbonization and the release of most volatiles with elevating the temperature from 300 to 550°C.These observations were also confirmed by the BET N$_2$ adsorption/desorption assays and BJH pore-size distribution of different biochars (Figure 1(a)), implying the presence of mesopores and micropores. The pore-size distribution of BC 300–400°Cwas within the 2–50 nm range, denoting a mesoporous material classification. The pore-size of biochars BC 450–550°C obeyed the micropores region (< 2 nm). Based on the aforementioned results, a high pyrolysis temperature would develop the biochar surface area, i.e., an essential property for entrapping high amounts of molecules via the pore-filling mechanism [26]. Additionally, an increase in pyrolysis temperature would provide an appropriate condition for attaining a high ash content and a stable physicochemical quality, which complied with the study by Song and Guo [30].

3.1.3. XRD Pattern.

The crystallinity of biochars synthesized at different pyrolysis temperatures was estimated using the XRD analysis (Figure 1(b)). The XRD patterns of biochars BC 300–550°C exhibited the predominance of two main crystalline minerals, i.e., quartz (SiO$_2$) and calcite (CaCO$_3$). Similarly, Kraiem et al. [17] indicated the occupancy of quartz and calcite in biochar prepared from the pyrolysis of waste fish fats at a temperature of 500°C. The XRD peaks observed at 2θ approximately of 20.9°, 36.6°, 50.2°, and 60.0° could be associated with (100), (110), (112) and (121) planes of SiO$_2$, respectively [13]. This result suggests that SiO$_2$ was the main crystalline phase for all biochars pyrolyzed throughout the temperature 300–550°C range. Some peaks of quartz for BC450–550 were higher than those for BC300–400, indicating the increment of quartz crystallization in biochars when the heating temperature increased. However, the peak intensities of calcite decreased with an increase in temperature, which could be due to decomposing carbonaceous materials (calcite) after thermal treatment with elevated temperatures [26]. The presence of calcite in all biochar samples would elucidate the pH distribution within the alkaline range (Table 1), as previously recognized by Yuan et al. [34]. Similarly, Fidel et al. [10] demonstrated that the intensities of XRD peaks ascribed to the mineral content (e.g., sylvite, calcite, and dolomite) of biochar were diminished under a high thermal treatment condition.

3.1.4. FTIR and Functional Groups.

Figure 1(c) shows the functional groups on the biochar surface treated at variouspyrolysistemperatures (300–550°C). The intensity of peaks between 3270 and 3380 1/cmdecreased largely withincreasing the pyrolysis temperature. This finding suggested that the organic O – H group was unstable at elevated temperatures, probably due to the biochar structure dehydration

[14]. Similarly, the reduction in peak intensities at 3250–3400 1/cm under higher temperature conditions could be associated with decomposing the organic nitrogen (N – H) groups in amines and amides. This finding could also explain the variation in the C/N ratio along with the pyrolysis temperature, as previously listed in Table 1. Thedominance of alkyl and oxygenated functional groups (e.g., C–O–C, COOH, −OH, and C=O)for BC300°C indicated that the biochar surface was more aliphatic at lower pyrolysis temperature. However, the structures of BC400–550°C were more aromaticat higher pyrolysis temperature (>400°C) because of the dehydroxylation and volatilization process, supporting crystallization [20]. Again, this finding complied with the XRD pattern (Figure 1(b)), suggesting that biochars were more crystalline at higher pyrolysis temperatures. Hence, the arrangement of carbon structures was adjusted from aliphatic to aromatic, with raising the pyrolysis temperature from 300 to 550°C. Moreover, some adsorption bands between 2850 and 2950 1/cm for BC300–400°C were gradually disappeared at pyrolysis temperatures over 400°C dueto the instability of the aliphatic hydrocarbon (–CH$_x$) groups. The change in C=O stretching (around 1700 1/cm) with temperature could be ascribed to the formation of some conjugated aromatic carbonyl/carboxyl groups at exceeding the pyrolysis temperature over 300°C[39]. A slight change in the peak intensity at 1604 1/cm with elevating the pyrolysis temperature could be associated with the stability of conjugated aromatic ring stretching of C=C groups [22], viz., this observation also supports the decrease of O/C ratio (see Table 1). Moreover, the biochar surface would be more hydrophobic at elevated temperatures because of the evolvement of oxygen functional groups via gasification [20, 26]. Accordingly, the −OH, −NH, and – CH$_3$ groups were unstable, with a concomitant increase in aromaticity at elevated temperatures. The decrease in the polar functional groups for BC400–550°C revealed the establishment of a condensed and carbonized structure owing to higher mass loss (Figure 1(c)). The presence of more functional groups (Figure 1(d)) for EMBC, viz., alkane (CH$_2$ and CH$_3$bands), aromatic (C=C stretching), esters (S-OR) group, and alcohol (OH stretch andH-bonded), would be usefulto form interactions and complexations with the adsorbate compounds.

3.1.5. SEM.

Figure 2 shows the surface morphologies of the biochar samples (BC300–550°C). The SEM micrographs clearly indicated the development of irregular and uneven biochar surfaces with channels and well-defined and vacant pores. A smooth textureand incomplete decomposition were noticed for BC300 – 400°C. However, the surfaceroughness and intensity increased for BC450 – 550°C, suggesting an improved porosity. This finding could be ascribed to the release of volatiles during carbonization with elevating the pyrolysis temperature [37].

3.2. Toluene and Xylene (TX)Removals in Single-Solute System

3.2.1. Effect of pH on TX Adsorption.

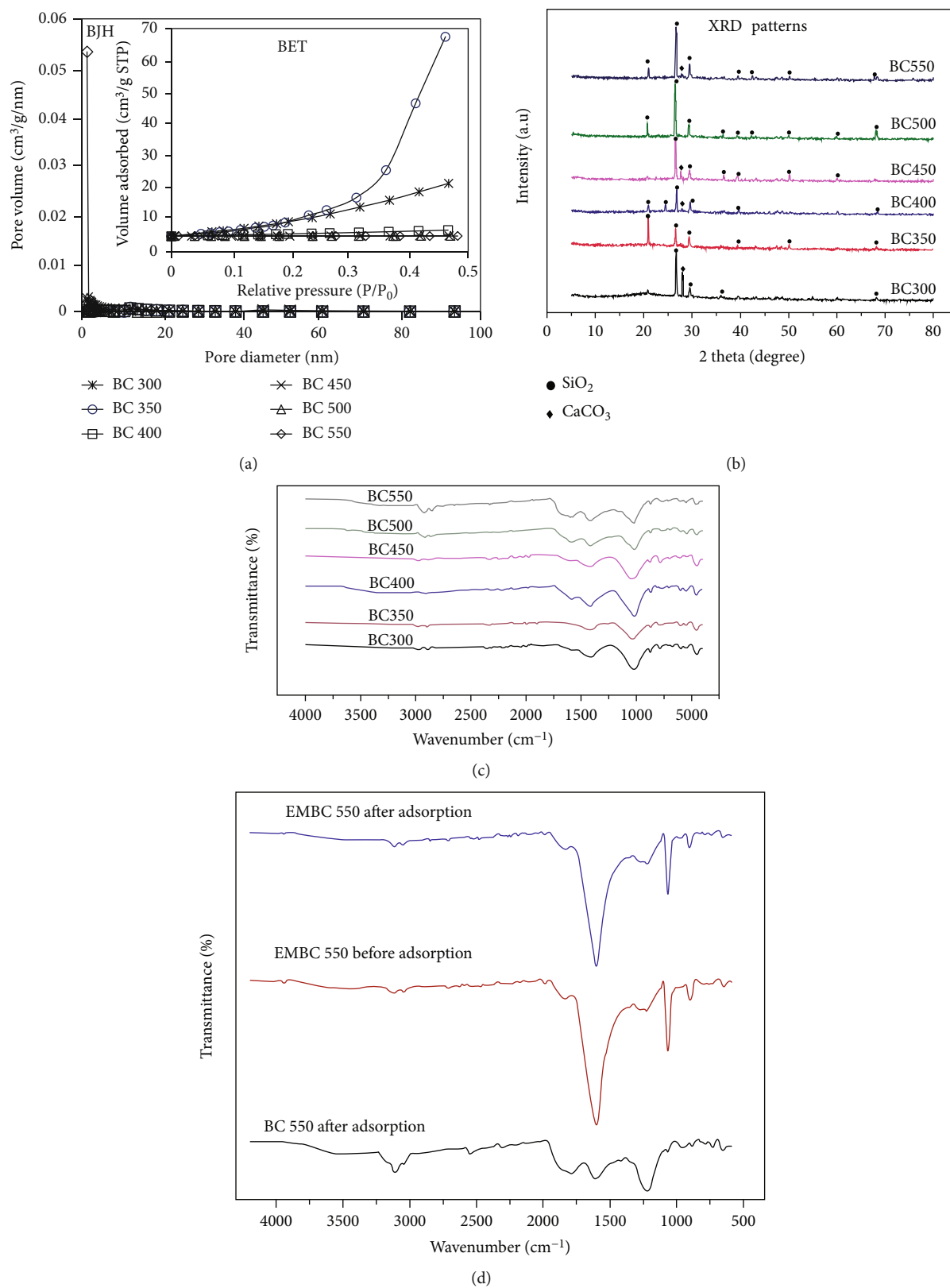Figure 3(a) shows the influence of solution pH on TX adsorption by biochars

FIGURE 1: Biochar adsorbent characterization: (a) BET nitrogen adsorption/desorption isotherms and BJH pore-size distribution, (b) XRD patterns of BC 300–550°C, (c) FTIR spectra of BC 300–550°C before adsorption, and (d) FTIR spectra of BC 550°C and EMBC 550°C after adsorption.
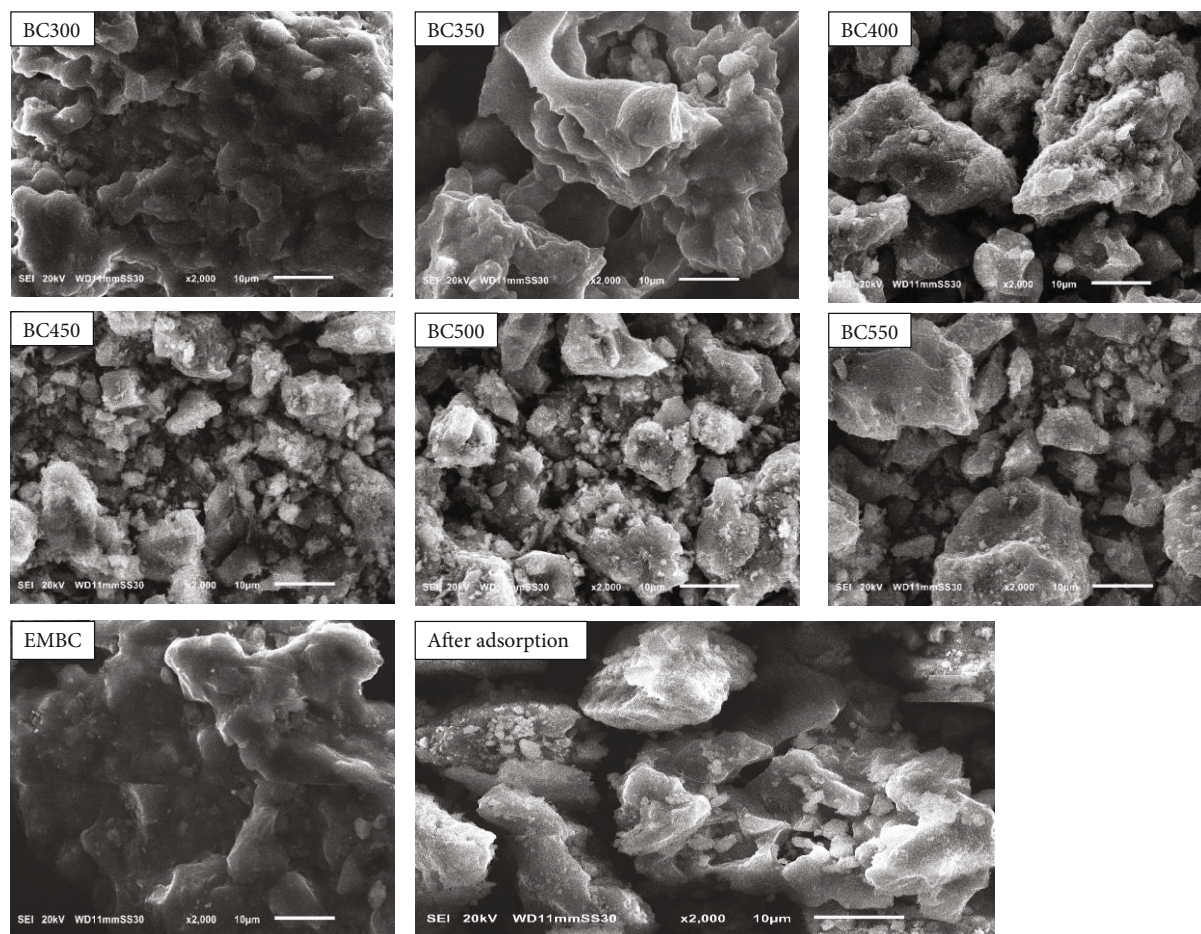
FIGURE 2: SEM of biochar and modified biochar adsorbents prepared under different pyrolysis conditions (300–550˚C).

(BC and EMBC). For BC, the T removal efficiency improved from 46.8 to 75.1%, with an increase in the solution pH from 2 to 10, respectively, suggesting that pH around 10 was favourable for the adsorption process. At the pH 10 condition, the X removal efficiency was comparable toT and reached 73.4%. The EMBC adsorbent attained better adsorption capabilities compared with BC, exhibiting the highest removal efficiencies of82.1% for T and 86.1% for X. At lower pH, the high concentration and mobility of H^+ ions tended to generate extremely protonated sorption sites [9], causing electrostatic repulsion to hinder the TX uptake ability. The data in Figure 3(a) also revealed that a further increase in solution pH over 10 caused an insignificant ($p > 0.01$) enhancement in the removal efficiencies of the TX adsorbate. This result could be ascribed to the competition between the adsorbate molecules and hydroxide (OH^-) ions for the active sites occupying the biochar surface [21]. The point of zero charge (pH_{PZC}) also showed a zero electrical charge density on the biochar surface at a solution pH of about 10 (Supplementary Figure S1). In another study, Jayawardhana et al. [15] found that pH conditions of 8.3 and 9.0 were favorable for the adsorption of toluene and m-xylene onto biochar prepared from municipal solid waste.

The affinity of EMBC towards TX adsorption over a wide pH scalecould be ascribed to the increase in the degree of ionization of surface functional groups (see Figure 1(d))

essential for binding the hydrophobic TX compounds with the biochar adsorbent. Moreover, the TX removalsundervarious pH conditions implied the occurrence of additionaladsorption mechanisms such as π-π bonding interaction and hydrophobic interaction [37].

3.2.2. Effect of Biochar Dosage on TX Adsorption. Figure 3(b) represents the influence of biochar dosage on TX removal by BC and EMBC. The removal efficiencies were improved from 77.8 to 84.1% for T and from 80.2 to 87.8% for X with increasing the EMBC dosage from 2 to10 g/L, respectively. These efficiencies were higher than the adsorption patterns attainedusing the unmodified BC biochar. The increase in the number of active adsorption sites on biochars, following the increment in biochar dosage, tended to uptake additional amounts of TX molecules [31]. Due to the insignificant ($p > 0.05$) variation in the TX removal efficiencies within the range of biochar dosage investigated, 2 g/L was selected for further investigations. This selection would minimize the requirement of chemical regeneration, disposal of exhausted adsorbents, and operational and maintenance issues.

3.2.3. Effect of Initial Concentration (C_o) on TX Adsorption. Figure 3(c) shows the effect of C_o on TX adsorption at the optimum factors (pH =10, biochar dosage =2 g/L, and time = 60 min). For the EMBC adsorbent, an increase in
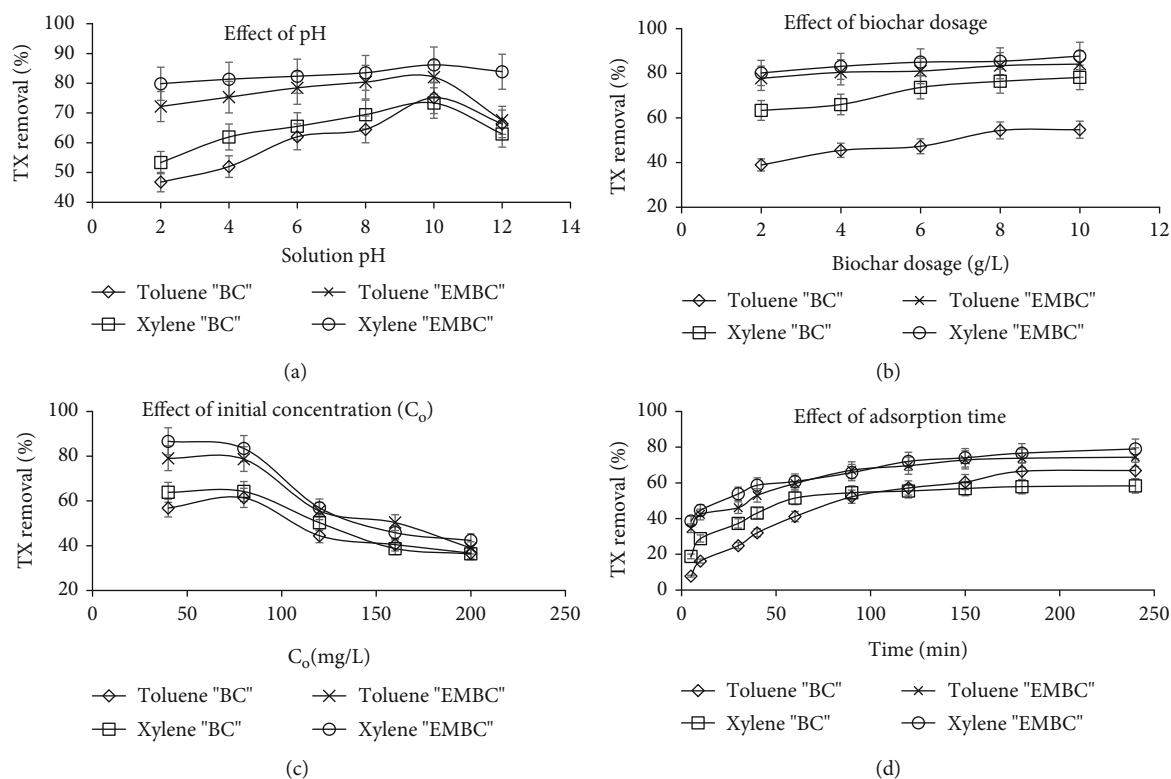
FIGURE 3: Effect of operational conditions on toluene and xylene (TX) removal efficiencies: (a) solution pH, (b) biochar dosage, (c) initial TX concentration, and (d) adsorption time.

C_o from 40 to 200 mg/L, respectively, caused a significant ($p < 0.05$) drop in the removal efficiencies of T from 79.1 to 39.0% and X from 86.6 to 42.4%. These data were better than the removal efficiencies observed when using raw BC biochars as an adsorbent material (Figure 3(c)). The negative correlation between the TX removal efficiency and C_o could be ascribed to the low ratio of adsorption sites-to-TX molecules (or the full occupancy of the available adsorption sites) at elevated C_o [3]. Moreover, the active binding sites of biochars would be saturated with an increase in the TX concentrations [33], suggesting that the removal efficiencies of the TX molecules by biochars were dependent on the C_o 40–200 mg/L range.

3.2.4. Effect of Adsorption Time on TX Adsorption. Figure 3(d) shows the effect of adsorption time on the removal percentage of TX by biochars (BC and EMBC) at pH = 10 and dosage = 2 g/L. For the EMBC material, the removal efficiencies of T and X were 69.6 and 72.1% at adsorption time = 120 min, respectively. These removal efficiencies were insignificantly ($p > 0.05$) improved to 74.4 and 79.0%, respectively, with an additional increase in adsorption time to 240 min. The rapid enhancement in TX adsorption within the initial 120 min could be ascribed to the accessibility of large amounts of vacant active sites [35]. The slight increase in the removal efficiencies after 120 min could be attributed to (i) a reduction in the number of vacant active sites of biochars [5], and (ii) a formation of repulsion between the adsorbate molecules [15]. A fast

removal rate, followed by a reduced pattern indicated a two-step adsorption process [33].

These results depicted that the equilibrium condition for adsorbing TX onto biochars would occur after a contact time of 120 min. A longer equilibrium time of 24 h was reported for the adsorption of T and X onto zeolite Na-P1, with removal efficiencies of 55% and 77–99%, respectively [5]. Jayawardhana et al. [15] found that about 5 h was suitable to attain an equilibrium time for adsorbing toluene and *m*-xylene by municipal solid waste biochar.

3.2.5. Adsorption Mechanisms. The results of adsorption isotherms revealed that the TX adsorbates were strongly attached to the EMBC surface via higher binding energy, as compared with BC (supplementary Figure S2; Table S1). Moreover, X had a better adsorption intensity or degree of favorability for adsorption than T. The TX molecules would form a uniform monolayer on the biochar surface within specific sites having equivalent sorption energy. In addition, all binding sites on biochars have equal affinity for the TX sorbate.

The adsorption favourability followed the order of X > T, and X needed a shorter time than T to attain a specific fractional uptake (supplementary Figure S3; Table S2). This pattern could be linked to an increase in both molecular weight (X 106.17 g/mol > T 92.14 g/mol) and hydrophobicity (X 2.77 – 3.15 > T 2.69), and a decrease in water solubility (X 175 – 198 mg/L < T 515 mg/L) [5]. A similar arrangement of adsorption favourability was established for the adsorption of
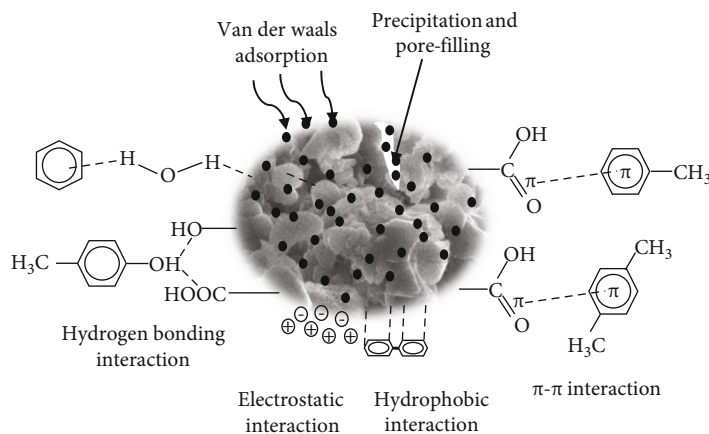
FIGURE 4: Possible mechanisms for adsorption of TX onto biochars.

TX ontosilica-based adsorbents [24] and multiwall carbon nanotubes [4]. Moreover, a higher affinity for X removal could be associated with the presence of two methyl groups connected to the benzene ring, augmenting the interaction with the biochar surface [16]. The reusability and recyclability of TX-loaded biochars were attained for five consecutive adsorption-desorption cycles (supplementary Figure S4).

According to the overall observation above, the adsorption of TX onto biochars could be graphically represented by Figure 4.

These adsorption mechanisms, occurring either in series or in parallel, could be summarized as follows:

(a) Monolayer adsorptiononto nearly homogenous binding sites, and no interaction would occur among adsorbate species, as revealed by the high fitting accuracy of the Langmuir isotherm model (see supplementary Figure S2 and Table S1).

(b) Precipitation and pore-filling, as depictedby the physical properties of adsorbents having many pores of different sizes (micropores and mesopores) (Table 1 and Figures 1 and 2).

(c) Electrostatic interactions due to the significant influence of solution pHon TX removal (Figure 3(a)), and the corresponding variation in electric charges (solution pH vs. biochar pH_{PZC}).

(d) Hydrogen bonding interaction with carboxyl and ester carbonyl groups of biochars

(e) π-π dispersive interaction between carboxylic oxygen-atom of biochar (electron-donor) and the aromatic ring of TX (electron-acceptor).

(f) Van der Waals sorption interaction between TX aromatic ring and electron-donating functional groups, as depicted by the surface functional group changes after adsorption (Figure 1(d)).

(g) Multiple diffusion mechanisms (surface/porediffusions), as revealed by thekinetic model parameters (see supplementary Figure S3; Table S2).

(h) A minor contribution of chemisorption

3.3. Real Petrochemical Wastewaterapplication.
The treatment of real PIW by biochars is an essential step towards the practical use of sludge-based adsorbents for industrial-scale applications. Wastewater samples collected from a petrochemical industry were composed of TOC = 127.4 ± 6.1 mg/L, benzene = 94.1 ± 4.6 mg/L, T = 340.2 ± 13.0 mg/L, ethylene = 457.0 ± 32.0 mg/L, and X = 55.2 ± 3.4 mg/L, representing a multi (competitive) aqueous solution. After the first adsorption cycle, the reductions of TOC, benzene, T, ethylene, and X denoted C/C_o = 0.61, 0.66, 0.61, 0.78, and 0.61, respectively, within 60 min (Figure 5(a) - 5(e)). Further, the EMBC material was regenerated and subjected to PIW (i.e., second cycle within60 min). TheC/C_o values were changed to 0.67, 0.73, 0.64, 0.80, and 0.66, respectively, suggesting a slight decline in the adsorption performance. After five regeneration cycles, the removal efficiencies of TOC, benzene, T, ethylene, and X decreased by 51.6%, 58.3%, 43.9%, 66.6%, and 48.8%, respectively. The decline in the biochar adsorption performance along with the successive adsorption/regeneration cycles could be ascribed to (i) the loss of the adsorbent active binding sites, and/or (ii) the presence of multiple anions and cations in the real-world industrial discharges [3, 24]. With a goodregeneration ability, this high adsorption capacity validates the application of biochar-based adsorption as a tertiary treatment phase for real PIW.

3.4. Application Prospects and Cost Estimation.
The environmental and economic aspects relating to the adsorption system were described for both BC and EMBC to determine the feasibility and cost-effectiveness of the adsorbent material. The cost estimation was derived as reported byHamdy et al. (2019) and Mahmoud et al. [21]. The calculations in Table 2 were represented with a precision of ±10% due to variations in local currency among countries used for assumptions.

3.4.1. Total Capital Investment (TCI).
The total capital investment (TCI) refers tothe sum of money spent on buildings and equipment to establish the project objectives [36]. TCI can be calculated in terms of fixed capital cost (FCC)
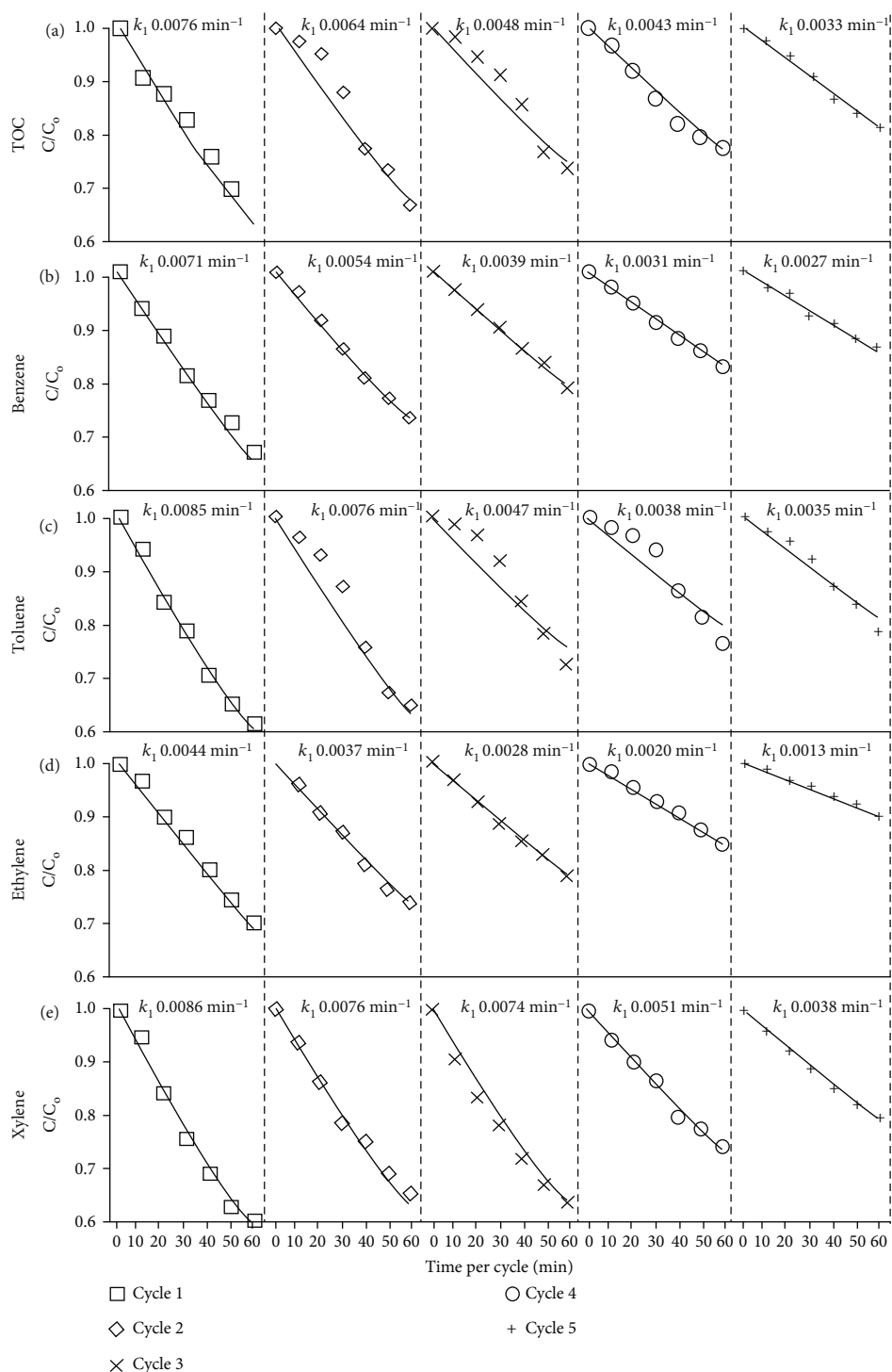
FIGURE 5: Performance of EMBC for treating real petrochemical effluents under five successive adsorption/regeneration cycles.

and working capital cost (WCC). As listed in Table 2, FCC was presumed regarding the land footprint, building of the offices and laboratories, electro-mechanical equipment, and piping and fitting, as reported by Elhafez et al. [7]. The low land and building costs were assigned to the financial support of the local government, attaining a "Waste Recycling" program. The equipment cost of EMBC was higher than that of BC due to the use of additional machines for handling,

washing, drying, and crushing the eggshell waste [29]. The installation and construction processes were estimated as 50% of the equipment cost. Accordingly, the FCC values were 4.20 USD/m^3 for BC and 5.60 USD/m^3 for EMBC. The WCC of the project was assigned to 6.5% of the FCC and regeneration costs, denoting the financing expenses used to run the adsorption process on a daily basis. Hence, the WCC values used to maintain the daily operations were

TABLE 2: Primary techno-economic estimation for producing biochars to treat wastewater-containing aromatic hydrocarbons, with ±10% precision.

Item	BC	EMBC	Unit
Calculation of total capital investment (TCI) in USD/m^3			
Building and construction	0.97	1.23	USD/m^3
Equipment purchase and installation	1.51	2.02	USD/m^3
Instrumentation and control	0.71	0.90	USD/m^3
Electrical system	0.67	1.01	USD/m^3
Piping system	0.34	0.45	USD/m^3
Fixed capital cost (FCC)	4.20	5.60	USD/m^3
Regeneration and recycling system	2.10	2.80	USD/m^3
Working capital cost (WCC)	0.41	0.55	USD/m^3
Total capital investment (TCI)	6.71	8.95	USD/m^3
Calculation of annual operation cost (AOC) in USD/m^3/yr			
Raw material and chemicals	0.17	0.23	USD/m^3/yr
Waste generation and disposal	0.23	0.29	USD/m^3/yr
Utilities (water and electricity)	0.25	0.31	USD/m^3/yr
Extra cost	0.22	0.30	USD/m^3/yr
Maintenance	0.08	0.11	USD/m^3/yr
Insurance	0.04	0.06	USD/m^3/yr
Annual operation cost (AOC)	0.98	1.30	USD/m^3/yr
Calculation of net profit (NP in USD/m^3/yr) and payback period (years)			
Annual profitability and revenue	1.49	2.48	USD/m^3/yr
Benefits of tertiary treated wastewater	0.23	0.36	USD/m^3/yr
Net profit (NP)	0.74	1.54	USD/m^3/yr
Tax	0.11	0.23	USD/m^3/yr
Net profit (after tax)	0.62	1.30	USD/m^3/yr
Payback period = TCI/net profit (after tax)	10.74	6.86	Years

0.41 USD/m^3 for BC and 0.55 USD/m^3 for EMBC. In this regard, the synthesis of BC and EMBC adsorbents entailed TCI values of 6.71 and 8.95 USD/m^3, respectively. A higherTCI of EMBC could be linked to the additional preparation procedures, including washing, drying/heating, and milling/sieving steps.

3.4.2. Annual Operation Cost (AOC). The annual operation cost (AOC) was estimated on a yearly basis, concerning raw material, utilities, operating labor, laboratory cost, maintenance and repair, and necessary extra costs [36]. The components of AOC were derived based on an operating time of 336 days per year, viz., 8-h shifts per day, 7 days per week, and 48 weeks per year, including 5 weeks for maintenance. The cost of raw material depended on sewage sludge and eggshells required for the pyrolysis process, as well as reagents (e.g., about 9 USD for each liter of H_2SO_4 95% and 10 USD for each kg of pure NaOH) [29]. The sewage sludge is not always available for free, and the chemicals were purchased from local chemical suppliers. Table 2 also lists the cost of utilities, including tariff levels of 0.12 USD/m^3 for water supply and 0.03 USD/kWh for electricityrequirement [9]. The operators and workers earned low hourly wages as the adsorption process is relatively simple and requires little experiencefor operation [12]. Extra costs

include adsorbent regeneration and recycling, and waste released during the preparation process. The maintenance and insurance expenses required for the regular repairing of damages were equivalent to 2% and 1% of FCC, respectively. According to the above calculations and data obtained from previous studies, the AOC of 0.98 USD/m^3/y for BC and 1.30 USD/m^3/y for EMBC could be determined.

3.4.3. Net Profit and Payback Period. The annual revenue could be obtained from selling the adsorbent material for removing toxic species with high concentrations [36]. The annual profitability should also includethe prices paid by the municipality to treat industrial wastewater, avoiding negative environmental consequences from releasing the contaminants via uncontrolled pathways [9]. Referring to the real market and contacts with potential customers, the EMBC price could reach up to 0.32 USD/kg compared with 0.15 USD per kg of BC for industrial applications. These prices could be compared with 0.09–0.33, 0.60, and 1.50 USD/kg forwood biochar, zeolite, and activated carbon, respectively [27]. The estimated values corresponded to a cost of about 8 USD to eliminate 1 kg of TX pollutantsfrom the environment (i.e., calculated from dividing the adsorbent price in USD/kg by adsorption capacity in mg/g). Hence, the net profit (NP) values were 0.74 and 1.54 USD/m^3/y for BC

TABLE 3: Possible achievement of SDGs relevant to the study outputs.

SDG	Description
Goal 2: Zero hunger	Biochar can improve agricultural soil fertility and facilitate soil carbon sequestration, increasing crop productivity. This advantage is essential to ensure sustainable food production systems and raise the incomes of small-scale food suppliers.
Goal 6: Clean water and sanitation	Biochar can be applied in wastewater treatment by eliminating (or immobilizing) heavy metals, dyes, oils, and organic and inorganic pollutants from aqueous solutions. This benefit would protect and restore water-related ecosystems, improve decentralized wastewater treatment systems, minimize nutrient leaching during irrigation, and enhance the sanitation in rural communities.
Goal 7: Affordable and clean energy	The elevated carbon content in biochar increases the energy value compared with traditional cooking fuels (e.g., firewood). Moreover, energy and synthetic gas are typically generated during biochar production. Hence, biochar could be an ideal alternative source of energy, especially for remote areas with limited electricity access [11].
Goal 9: Industry, innovation and infrastructure	Biochar synthesized from pyrolysis can act as direct catalysts in various industrial applications, which have been covered by Lee et al. [19]. These applications have also been outlined by the Biochar Industry Technology Innovation Strategic Alliance of China-BITISAC.
Goal 13: Climate action	Generally, N-based fertilizers are associated with N_2O emissions. Hence, the biochar application in agricultural fields to reduce excessive fertilizers would mitigate the GHG emission.
Goal 14: Life below water	According to the biochar-goal 6 description, biochar has additional benefits in protecting marine and coastal ecosystems from pollution (i.e., enriching life in water).

and EMBC, respectively. Further, the adsorption process was economically evaluated using the payback period; i.e., a general criterion obtained from TCI divided by NP. The payback periods (after 15% local tax) were 10.7 years for BC and 6.9 years for EMBC. These periodsare shorter than theproject lifetime (i.e., 15 years), signifying a profitability scheme. In addition, the payback period of EMBC wasshorter than that of BC because the modified biochar-related project would recover its initial investment rapidly.

3.5. Sludge-Based Biochar Technology for Meeting Sustainable Development Goals (SDGs). The increasingly stringent environmental regulations have strongly imposed the researchers to find viable and economically feasible scenarios for industrial effluent treatment. Table 3 summarizes the number of SDGs that could be relevant to the study objectives. In this work, the EMBC adsorbent showed appropriate PIW treatment under repeated adsorption-regeneration (five) cycles, expressing a good reusable and recycling ability for industrial applications. This property would reduce the environmental risks caused by industrial effluents; hence, goal 6 (Clean Water and Sanitation) and goal 14 (Life below Water) could be partially achieved. The study also represented the utilization of material of natural origin (eggshells) for synthesizing biochar with unique properties, such as a low O/C ratio (see Table 1). Hence, no toxic chemicals or reagents were used during preparation, implying that biochar would act as a competitive and sustainable resource. The prepared biochar would have other applications such as soil quality improvement, catalysts, additives for anaerobic digestion/composting, and reducing GHG emissions. These applications have been comprehensively reviewed by Zhang et al. [38]. The public should have adequate education, skills, and awareness about the potential human health, socio-economic, and environmental advantagesassociated with biochar production. Proper mass media, advertisements, and programs should transfer the understanding of biochar-based projects to the

public sector, especially in developing countries. The social benefit relevant to achievable SDGs should ensure jobs creation, awareness, education, and the standard of living.

3.6. Progress and Future Perspectives. Because the reusability of exhausted biochars is essential under real PIW wastewater applications, further studies are required to develop a convenient and economical regeneration method. Various thermal, biological, micro-wave, and ultrasound methods could be used to enhance the biochar regeneration process by liberating the complex organic contaminations. Several parameters, such as breakthrough time, desorption cycles and capacity, and bed exhaustion time, should be optimized to improve the regeneration efficiency. Moreover, the solvent used as an eluting agent for biochar regeneration should be appropriately selected based on its concentration, volume, and preferable pH condition, improving the economic viability of the adsorption/desorption cycles. The ability of biochars to eliminate other compounds in PIW such as ethylene glycol, formaldehyde, tetrachloroethylene, and 1,3-butadiene by adsorption should be further investigated.

4. Conclusions

The current worksuccessfully synthesized and characterized sludge-based biochars having high aromaticity, carbonization degree, and quartz crystallization. Biochar adsorbent showed high performance for removing toluene and xylene pollutants with efficiencies of 79.1% and 86.6% at solution pH =10, biochar dosage of 2 g/L, and C_o =40 mg/L within 60 min. The proposed adsorption mechanism also revealed a high ability to remove petroleum hydrocarbons from both synthetic and real PIW. Moreover, the synthesized biochar exhibited an economic benefit for industrialization with a payback period = 6.9 yr. The interlinkagesbetween PIW treatment and SDGs (e.g., SDG 3, SDG 6, SDG 9, and SDG 14) were identified via (i) reducing the environmental risks

caused by industrial effluents, (ii) utilizing eggshell residues and sewage sludge for biochar preparation, avoiding waste disposal issues, (iii) synthesizing a cost-effective EMBC adsorbent showing a twofold increase in the specific surface area than conventional biochars, improving biochar production technology, and (iv) raising public awareness about waste management.

Data Availability

All data generated or analyzed during this study are included in this published article, and its supplementary information files.

Conflicts of Interest

The authors declare that they have no known competing financial interests or personal relationships that could have appeared to influence the work reported in this paper.

Authors' Contributions

AGK: Methodology, Formal analysis, Writing - original draft; MGI: Conceptualization, Visualization, Writing - review & editing; MF: Supervision, Visualization, Writing - review & editing; MN: Conceptualization, Supervision, Writing - review & editing.

Acknowledgments

Supplementary Materials

Supplementary figures and tables illustrate(i) points of zero charge (pH_{pzc}) of the biochar adsorbents, (ii) studies of Langmuir and Freundlich adsorption isotherms, (iii) studies ofPseudo-first-order, Pseudo-second-order, and intraparticle diffusion (IPD) model kinetics, and (iv)regeneration of biochars. (Supplementary Materials)

References

[1] M. Abdel-Aziz, S. Younis, Y. Moustafa, and M. Khalil, "Synthesis of recyclable carbon/lignin biocomposite sorbent for _in-situ_ uptake of BTX contaminants from wastewater," Journal of Environmental Management, vol. 233, pp. 459–470, 2019.

[2] M. Ahmad, S. S. Lee, X. Dou et al., "Effects of pyrolysis temperature on soybean Stover- and peanut shell-derived biochar properties and TCE adsorption in water," Bioresource Technology, vol. 118, pp. 536–544, 2012.

[3] L. Alamo-Nole, O. Perales-Perez, and F. Roman-Velazquez, "Sorption study of toluene and xylene in aqueous solutions by recycled tires crumb rubber," Journal of Hazardous Materials, vol. 185, no. 1, pp. 107–111, 2011.

[4] H. Anjum, K. Johari, N. Gnanasundaram, A. Appusamy, and M. Thanabalan, "Investigation of green functionalization of multiwall carbon nanotubes and its application in adsorption of benzene, toluene & p-xylene from aqueous solution," Journal of Cleaner Production, vol. 221, pp. 323–338, 2019.

[5] L. Bandura, D. Kołodyńska, and W. Franus, "Adsorption of BTX from aqueous solutions by Na-P1 zeolite obtained from fly ash," Process Safety and Environmental Protection, vol. 109, pp. 214–223, 2017.

[6] J. Carvalho, J. Araujo, and F. Castro, "Alternative low-cost adsorbent for water and wastewater decontamination derived from eggshell waste: an overview," Waste and Biomass Valorization, vol. 2, no. 2, pp. 157–167, 2011.

[7] S. Elhafez, H. Hamad, A. Zaatout, and G. Malash, "Management of agricultural waste for removal of heavy metals from aqueous solution: adsorption behaviors, adsorption mechanisms, environmental protection, and techno-economic analysis," Environmental Science and Pollution Research, vol. 24, no. 2, pp. 1397–1415, 2017.

[8] Y. Fatimah, K. Govindan, R. Murniningsih, and A. Setiawan, "Industry 4.0 based sustainable circular economy approach for smart waste management system to achieve sustainable development goals: A case study of Indonesia," Journal of Cleaner Production, vol. 269, article 122263, 2020.

[9] M. Fawzy, M. Nasr, A. M. Abdel-Rahman, G. Hosny, and B. R. Odhafa, "Techno-economic and environmental approaches of Cd2+adsorption by olive leaves (Olea europaeaL.) waste," International Journal of Phytoremediation, vol. 21, no. 12, pp. 1205–1214, 2019.

[10] R. Fidel, D. Laird, M. Thompson, and M. Lawrinenko, "Characterization and quantification of biochar alkalinity," Chemosphere, vol. 167, pp. 367–373, 2017.

[11] W. Gwenzi, N. Chaukura, F. N. D. Mukome, S. Machado, and B. Nyamasoka, "Biochar production and applications in sub-Saharan Africa: opportunities, constraints, risks and uncertainties," Journal of Environmental Management, vol. 150, pp. 250–261, 2015.

[12] A. Hamdy, M. Mostafa, and M. Nasr, "Techno-economic estimation of electroplating wastewater treatment using zero-valent iron nanoparticles: batch optimization, continuous feed, and scaling up studies," Environmental Science and Pollution Research, vol. 26, no. 24, pp. 25372–25385, 2019.

[13] Z. Han, B. Sani, W. Mrozik et al., "Magnetite impregnation effects on the sorbent properties of activated carbons and biochars," Water Research, vol. 70, pp. 394–403, 2015.

[14] M. Hossain, V. Strezov, K. Y. Chan, A. Ziolkowski, and P. F. Nelson, "Influence of pyrolysis temperature on production and nutrient properties of wastewater sludge biochar," Journal of Environmental Management, vol. 92, no. 1, pp. 223–228, 2011.

[15] Y. Jayawardhana, S. R. Gunatilake, K. Mahatantila, M. P. Ginige, and M. Vithanage, "Sorptive removal of toluene and m-xylene by municipal solid waste biochar: simultaneous municipal solid waste management and remediation of volatile organic compounds," Journal of Environmental Management, vol. 238, pp. 323–330, 2019.

[16] N. Klomkliang, D. Do, and D. Nicholson, "Affinity and packing of benzene, toluene, andp-Xylene adsorption on a graphitic surface and in pores," Industrial and Engineering Chemistry Research, vol. 51, no. 14, pp. 5320–5329, 2012.

[17] T. Kraiem, A. Ben Hassen-Trabelsi, S. Naoui, and H. Belayouni, "Characterization of syngas and bio-char: co-products from pyrolysis of waste fish fats," in IREC 2014 - 5th International Renewable Energy Congress, Hammamet, Tunisia, 2014.

[18] A. Kumi, M. Ibrahim, M. Fujii, and M. Nasr, "Synthesis of sludge-derived biochar modified with eggshell waste for monoethylene glycol removal from aqueous solutions," *SN Applied Sciences*, vol. 2, no. 10, 2020.

[19] J. Lee, K.-H. Kim, and E. Kwon, "Biochar as a catalyst," *Renewable and Sustainable Energy Reviews*, vol. 77, pp. 70–79, 2017.

[20] D.-C. Li and H. Jiang, "The thermochemical conversion of non-lignocellulosic biomass to form biochar: A review on characterizations and mechanism elucidation," *Bioresource Technology*, vol. 246, pp. 57–68, 2017.

[21] A. Mahmoud, M. Mostafa, and M. Nasr, "Regression model, artificial intelligence, and cost estimation for phosphate adsorption using encapsulated nanoscale zero-valent iron," *Separation Science and Technology (Philadelphia)*, vol. 54, no. 1, pp. 13–26, 2019.

[22] T. Mimmo, P. Panzacchi, M. Baratieri, C. A. Davies, and G. Tonon, "Effect of pyrolysis temperature on miscanthus (Miscanthus × giganteus) biochar physical, chemical and functional properties," *Biomass and Bioenergy*, vol. 62, pp. 149–157, 2014.

[23] M. Naderi, "Surface area: Brunauer–Emmett–Teller (BET)," in *Progress Infiltration and Separation*, E. S. Tarleton, Ed., pp. 585–608, Academic Press, 2014.

[24] T. Ncube, K. S. K. Reddy, A. Al Shoaibi, and C. Srinivasakannan, "Benzene, toluene, m-xylene adsorption on silica-based adsorbents," *Energy and Fuels*, vol. 31, no. 2, pp. 1882–1888, 2017.

[25] N. Ren, Y. Tang, and M. Li, "Mineral additive enhanced carbon retention and stabilization in sewage sludge-derived biochar," *Process Safety and Environmental Protection*, vol. 115, pp. 70–78, 2018.

[26] A. Shaaban, S.-M. Se, M. F. Dimin, J. M. Juoi, M. H. M. Husin, and N. M. M. Mitan, "Influence of heating temperature and holding time on biochars derived from rubber wood sawdust via slow pyrolysis," *Journal of Analytical and Applied Pyrolysis*, vol. 107, pp. 31–39, 2014.

[27] S. Shaheen, N. K. Niazi, N. E. E. Hassan et al., "Wood-based biochar for the removal of potentially toxic elements in water and wastewater: a critical review," *International Materials Reviews*, vol. 64, no. 4, pp. 216–247, 2019.

[28] J. Shi, X. Fan, D. C. W. Tsang et al., "Removal of lead by rice husk biochars produced at different temperatures and implications for their environmental utilizations," *Chemosphere*, vol. 235, pp. 825–831, 2019.

[29] B. Silva, M. Martins, M. Rosca et al., "Waste-based biosorbents as cost-effective alternatives to commercial adsorbents for the retention of fluoxetine from water," *Separation and Purification Technology*, vol. 235, article 116139, 2020.

[30] W. Song and M. Guo, "Quality variations of poultry litter biochar generated at different pyrolysis temperatures," *Journal of Analytical and Applied Pyrolysis*, vol. 94, pp. 138–145, 2012.

[31] P. Stähelin, A. Valério, S. M. . A. Guelli Ulson de Souza, A. da Silva, J. A. Borges Valle, and A. A. Ulson de Souza, "Benzene and toluene removal from synthetic automotive gasoline by mono and bicomponent adsorption process," *Fuel*, vol. 231, pp. 45–52, 2018.

[32] Y. Tang, M. S. Alam, K. O. Konhauser et al., "Influence of pyrolysis temperature on production of digested sludge biochar and its application for ammonium removal from municipal wastewater," *Journal of Cleaner Production*, vol. 209, pp. 927–936, 2019.

[33] H. Tran, S.-J. You, A. Hosseini-Bandegharaei, and H.-P. Chao, "Mistakes and inconsistencies regarding adsorption of contaminants from aqueous solutions: A critical review," *Water Research*, vol. 120, pp. 88–116, 2017.

[34] J.-H. Yuan, R.-K. Xu, and H. Zhang, "The forms of alkalis in the biochar produced from crop residues at different temperatures," *Bioresource Technology*, vol. 102, no. 3, pp. 3488–3497, 2011.

[35] F. Yu, J. Ma, and Y. Wu, "Adsorption of toluene, ethylbenzene and xylene isomers on multi-walled carbon nanotubes oxidized by different concentration of NaOCl," *Frontiers of Environmental Science and Engineering in China*, vol. 6, no. 3, pp. 320–329, 2012.

[36] Z. Yunus, A. al-Gheethi, N. Othman, R. Hamdan, and N. N. Ruslan, "Removal of heavy metals from mining effluents in tile and electroplating industries using honeydew peel activated carbon: A microstructure and techno- economic analysis," *Journal of Cleaner Production*, vol. 251, article 119738, 2020.

[37] L. Zhang, T. Xu, X. Liu, Y. Zhang, and H. Jin, "Adsorption behavior of multi-walled carbon nanotubes for the removal of olaquindox from aqueous solutions," *Journal of Hazardous Materials*, vol. 197, pp. 389–396, 2011.

[38] Z. Zhang, Z. Zhu, B. Shen, and L. Liu, "Insights into biochar and hydrochar production and applications: A review," *Energy*, vol. 171, pp. 581–598, 2019.

[39] Y. Zhao, D. Feng, Y. Zhang, Y. Huang, and S. Sun, "Effect of pyrolysis temperature on char structure and chemical speciation of alkali and alkaline earth metallic species in biochar," *Fuel Processing Technology*, vol. 141, pp. 54–60, 2016.